PERGAMON

International Journal of Heat and Mass Transfer 45 (2002) 15–23

International Journal of HEAT and MASS TRANSFER

www.elsevier.com/locate/ijhmt

Estimation of two-sided boundary conditions for two-dimensional inverse heat conduction problems

Han-Taw Chen [a,*], Sheng-Yih Lin [a], Hung-Ru Wang [a], Lih-Chuan Fang [b]

[a] *Department of Mechanical Engineering, National Cheng Kung University, Tainan 70101, Taiwan, ROC*

[b] *Chinese Military Academy, Fengshan, Kaoshiung 830, Taiwan, ROC*

Received 5 November 2000; received in revised form 12 April 2001

Abstract

A hybrid numerical algorithm of the Laplace transform technique and finite-difference method with a sequential-in-time concept and the least-squares scheme is proposed to predict the unknown surface temperature of two-sided boundary conditions for two-dimensional inverse heat conduction problems. In the present study, the functional form of the estimated surface temperatures is unknown a priori. The whole time domain is divided into several analysis sub-time intervals and then the unknown surface temperatures in each analysis interval are estimated. To enhance the accuracy and efficiency of the present method, a good comparison between the present estimations and previous results is demonstrated. The results show that good estimations on the surface temperature can be obtained from the transient temperature recordings only at a few selected locations even for the case with measurement errors. It is worth mentioning that the unknown surface temperature can be accurately estimated even though the thermocouples are located far from the estimated surface. Owing to the application of the Laplace transform technique, the unknown surface temperature distribution can be estimated from a specific time.

1. Introduction

Quantitative understanding of the heat transfer processes occurring in industrial applications requires accurate knowledge of internal heat sources, the thermal properties of the material or surface conditions. In practical situations these unknown quantities are to be determined from transient temperature measurements or transient displacement measurements at one or more interior locations. These measurements can be fitted and then the unknown quantities may be estimated. Such problems are called inverse problems which have become an attractive subject recently. To date, various methods have been developed for the analysis of the inverse heat conduction problems involving the estimation of surface conditions from measured temperatures inside the material [1–14]. However, most analytical and numerical methods were only employed to deal with one-dimensional inverse heat conduction problems (IHCP). Few works were presented for two- or three-dimensional IHCP because the difficulty of these problems was more pronounced.

The literature reviews showed that Sparrow et al. [2], Woo and Chow [3], Monde [4], Chen and Chang [13] and Chen et al. [14] have applied the Laplace transform method to predict the unknown surface conditions from temperature measurements only. It can be found that the methods proposed by Sparrow et al. [2] and Woo and Chow [3] were only limited to some simple linear inverse heat conduction problems. Their results have good accuracy only for short time. Thus their range of applications was limited. Imber [5] obtained an analytical solution of the two-dimensional IHCP. Other numerical methods for IHCP have been proposed including the dynamic programming method investigated by Busby and Trujillo [6], the finite element method applied by Krutz et al. [7], the boundary element method in conjunction with the Beck's sensitivity analysis and least-squares method presented by Zabaras and Liu [8]. Subsequent works of Yang and Chen [9], Yang

* Corresponding author. Fax: +886-6-296-6691.
E-mail address: htchen@mail.ncku.edu.tw (H.-T. Chen).

0017-9310/02/$ - see front matter
PII: S0017-9310(01)00138-7

Nomenclature

C_i	undetermined coefficient
F_1, F_2	estimated functions
$\{f\}$	force matrix
J	number of thermocouples
$[k]$	global conduction matrix
L	side length of a square plane plate
ℓ_x, ℓ_y	distance between two neighboring nodes in the x- and y-direction
M	number of discrete measurement times
n	number of measurements
n_x, n_y	number of nodes in the x- and y-direction
s	Laplace transform parameter
T	temperature
t	dimensionless time
t_f	dimensionless final time
x, y	dimensionless spatial coordinates

Greek symbols

α	thermal diffusivity
$\tilde{T}$	transformed dimensionless temperature
$\{\tilde{T}\}$	global dimensionless temperature matrix in the transform domain
σ^*	standard deviation of the mean
ω	averaged random error

[10,11] and Hsu et al. [12] applied the finite-difference method in conjunction with the linear least-squares method to estimate the one-sided and two-sided boundary conditions in two-dimensional IHCP. It is worth noting that the functional form of the estimated surface temperature is given a priori for these works and then the unknown surface temperature was parameterized. Thus a few measurement locations can be sufficient to estimate the unknown surface temperature. However, the effect of the measurement errors on the estimated surface temperature cannot be neglected.

Chen and Chang [13] have used the hybrid application of the Laplace transform technique and the finite-difference method to estimate the unknown surface temperature in one-dimensional IHCP using measured nodal temperatures inside the material at any specific time without measurement errors. Recently, Chen et al. [14,15] and Chen and Lin [16] applied the above scheme in conjunction with a sequential-in-time concept and the least-squares method to estimate the unknown surface conditions and thermal properties of the tested material from temperature measurements only. It can be observed from the work of Chen et al. [14] that the estimated surface temperatures are in good agreement with the exact results of the direct problem for various cases. To further demonstrate the accuracy and efficiency of the method proposed by Chen et al. [14] in estimating the surface temperature from temperature measurements, the present problem is investigated and a comparison between the present estimates and the results given by Yang [10] is also made. In performing the numerical simulation of the present study, the functional form of the surface temperatures is unknown a priori. The whole time domain is divided into several analysis sub-time intervals and then the surface temperatures in each analysis interval are estimated. The computational procedure for the estimation of the surface temperatures is performed repeatedly until the sum of the squares of the deviations between the calculated and measured temperatures is minimum.

In experiments, the measurement of temperature is, in general, somewhat inaccurate. This may be due to human error, but more often, it is due to inherent limitations in the equipment being used to make the measurements. The IHCP is typically sensitive to measurement errors. Equivalently, slight measurement errors can affect the accuracy of estimated surface conditions. Thus the effect of measurement errors on the estimation of the surface temperature will be investigated in the present analysis.

2. Mathematical formulation

A square plane plate with the length of the side L shown in Fig. 1 is considered. The initial temperature is T_0^*. For time $t^* > 0$, the boundaries at $x^* = 0$ and $y^* = L$ are kept insulated. For the direct heat conduction problem, the temperature field in the plane plate as a function of space and time can be determined provided that the surface temperatures at $x^* = L$ and $y^* = 0$ are

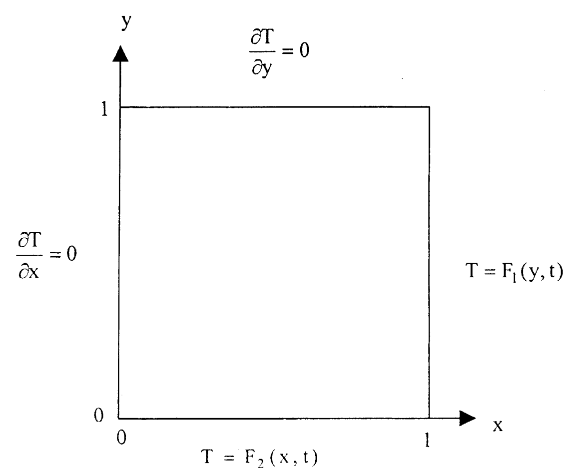

Fig. 1. Geometry of two-dimensional plane plate.

given. On the contrary, the surface temperatures at $x^* = L$ and $y^* = 0$ need to be estimated unless additional information on temperature in the slab is given. For convenience of numerical analysis, the following dimensionless parameters are introduced:

$$T = \frac{T^* - T_0^*}{T_0^*}, \quad x = \frac{x^*}{L}, \quad y = \frac{y^*}{L}, \quad t = \frac{\alpha t^*}{L^2}, \tag{1}$$

where T^* denotes the plate temperature. α is the thermal diffusivity of the plate.

In order to compare with the results of Yang [10], the dimensionless form of a two-dimensional heat conduction problem in the Cartesian coordinate system with the dimensionless parameters in Eq. (1), as shown in Fig. 1, is given by

$$\frac{\partial T}{\partial t} = \frac{\partial^2 T}{\partial x^2} + \frac{\partial^2 T}{\partial y^2} \quad \text{in } 0 < x < 1,\ 0 < y < 1, \quad 0 < t \leqslant t_f \tag{2}$$

with the dimensionless boundary conditions

$$T = F_1(y,t) \quad \text{at } x = 1, \tag{3}$$

$$T = F_2(x,t) \quad \text{at } y = 0, \tag{4}$$

$$\frac{\partial T}{\partial x} = 0 \quad \text{at } x = 0, \tag{5}$$

$$\frac{\partial T}{\partial y} = 0 \quad \text{at } y = 1, \tag{6}$$

and the dimensionless initial condition

$$T = 0 \quad \text{for } t = 0, \tag{7}$$

where t_f is the dimensionless final time for temperature measurements. The continuous surface temperature functions $F_1(y,t)$ and $F_2(x,t)$ in Eqs. (3) and (4) should be the time-and-space distribution. These unknown functions will be estimated from some interior temperature measurements.

To estimate the unknown functions $F_1(y,t)$ and $F_2(x,t)$, the additional information of discrete temperature measurements is required. Thus the temperature histories at some locations are measured in the plane plate. It is assumed that J thermocouples are used to record the temperature information at these selected locations, as shown in Table 1. The temperature histories taken from the thermocouples at successive specific dimensionless time t_m are denoted by $T_{i,m}^{\text{mea}}$, $i = 1, \ldots, J$, and $m = 1, \ldots, M$, where M denotes the number of the discrete measurement times. The temperature histories measured by these thermocouples will be used to estimate $F_1(y,t)$ and $F_2(x,t)$.

Because of experimental uncertainty, more realistic measurements should add simulated small random errors to the exact data, $T_{i,m}^{\text{exa}}$, obtained from the solution of the direct problem. Thus the measured data, $T_{i,m}^{\text{mea}}$, should be modified by adding small random errors to simulate experimental measurements. $T_{i,m}^{\text{mea}}$ used in the present inverse analysis can be expressed as

Table 1
Measurement locations of the present study and Yang [10]

Yang [10] (x,y)	Present study	
	Case A (x,y)	Case B (x,y)
(0.7, 0.2)	(0.7, 0.2)	(0.8, 0.8)
(0.8, 0.3)	(0.8, 0.3)	(0.2, 0.2)
(0.8, 0.2)	(0.6, 0.2)	(0.2, 0.4)
(0.6, 0.2)	(0.8, 0.4)	(0.6, 0.8)
(0.8, 0.4)	(0.8, 0.5)	(0.4, 0.8)
(0.8, 0.5)	(0.5, 0.2)	(0.2, 0.6)
(0.5, 0.2)		

$$T_{i,m}^{\text{mea}} = T_{i,m}^{\text{exa}}(1 + \omega), \quad m = 1, \ldots, M, \tag{8}$$

where ω represents the averaged random error and is assumed to be within −0.05 to 0.05 in the present study. σ^* is the standard deviation of the mean with respect to the exact data and is defined as [17]

$$\sigma^* = \left[\sum_{m=1}^{M} (T_{i,m}^{\text{mea}} - T_{i,m}^{\text{exa}})^2\right]^{1/2} \Big/ M, \quad i = 1, \ldots, J. \tag{9}$$

In real industrial applications, the actual measured profiles often exhibit random oscillations owing to measurement errors. Thus a polynomial function can be used to fit these measured data using the least-squares scheme [17].

In order to remove the time-dependent terms from the governing differential Eq. (2) and boundary conditions (3)–(6) with the initial condition (7), the method of the Laplace transform is employed [13–16,18,19].

The Laplace transform of a function $\phi(t)$ is defined as follows:

$$\tilde{\phi}(s) = \int_0^\infty \phi(t)\, e^{-st}\, dt, \tag{10}$$

where s is the Laplace transform parameter. The Laplace transform of Eqs. (2)–(6) gives

$$\frac{\partial^2 \tilde{T}}{\partial x^2} + \frac{\partial^2 \tilde{T}}{\partial y^2} - s\tilde{T} = 0 \quad \text{in } 0 < x < 1,\ 0 < y < 1 \tag{11}$$

and

$$\tilde{T} = \tilde{F}_1(y,s) \quad \text{at } x = 1, \tag{12}$$

$$\tilde{T} = \tilde{F}_2(x,s) \quad \text{at } y = 0, \tag{13}$$

$$\frac{\partial \tilde{T}}{\partial x} = 0 \quad \text{at } x = 0, \tag{14}$$

$$\frac{\partial \tilde{T}}{\partial y} = 0 \quad \text{at } y = 1. \tag{15}$$

The discretized forms of Eqs. (11)–(15) obtained by using the central-difference approximation, are, respectively, given as:

$$\frac{\tilde{T}_{j+1,k}+\tilde{T}_{j,k}+\tilde{T}_{j-1,k}}{\ell_x^2}+\frac{\tilde{T}_{j,k+1}+\tilde{T}_{j,k}+\tilde{T}_{j,k-1}}{\ell_y^2}=s\tilde{T}_{j,k}, \quad \mathrm{j}=1,2,\ldots,n_x,\ \ k=1,2,\ldots,n_y \tag{16}$$

and

$$\tilde{T}_{n_x,k}=\tilde{F}_1[(k-1)\ell_y,s],\quad k=1,2,\ldots,n_y, \tag{17}$$

$$\tilde{T}_{j,1}=\tilde{F}_2[(j-1)\ell_x,s],\quad j=1,2,\ldots,n_x, \tag{18}$$

$$\tilde{T}_{0,k}=\tilde{T}_{2,k},\quad k=1,2,\ldots,n_y, \tag{19}$$

$$\tilde{T}_{j,n_y-1}=\tilde{T}_{j,n_y+1},\quad j=1,2,\ldots,n_x, \tag{20}$$

where n_x and n_y indicate the number of nodes along the x- and y-direction, respectively. ℓ_x and ℓ_y, respectively designate the distance between two neighboring nodes in the x- and y-direction and are uniform. Their values are $\ell_x=1/(n_x-1)$ and $\ell_y=1/(n_y-1)$.

The rearrangement of Eqs. (16)–(20) gives the following vector-matrix equation.

$$[k]\{\tilde{T}\}=\{f\}, \tag{21}$$

where $[k]$ is an $n_x\times n_y$ matrix, $\{\tilde{T}\}$ is an $n_x\times 1$ matrix representing the unknown dimensionless nodal temperatures in the s domain and $\{f\}$ is an $n_x\times 1$ matrix. The Gaussian elimination algorithm and the numerical inversion of the Laplace transform [20] are applied to invert the temperature in the s domain $\tilde{T}$ to that in the physical quantity T. The advantage of the present method is that the estimation of the unknown surface temperatures at a specific time does not need to proceed with step-by-step computation from the initial measurement time t_0.

The unknown functions $F_1(y,t)$ and $F_2(x,t)$ are difficult to be fitted by a polynomial function for the whole time domain considered. Thus the time domain $t_0\leqslant t\leqslant t_f$ will be divided into some analysis intervals where t_0 is the initial measurement time. Owing to the application of the Laplace transform in the present study, t_0 is not always the initial time. This implies that the approximations of the unknown surface temperatures are carried out by discretizing the unknown functions $F_1(y,t)$ and $F_2(x,t)$ in Eqs. (3) and (4). Under this circumstance, a sequential-in-time procedure is introduced to estimate the unknown surface temperatures. Assume that the dimensionless measurement time step Δt_e is $\Delta t_e=(t_f-t_0)/M$. The discrete time coordinate t_m is $t_m=t_0+m\Delta t_e$ $(m=1,2,\ldots,M)$. Each of the analysis intervals in the present study is assumed to be $t_{m-1}\leqslant t\leqslant t_m$. In this work the polynomial forms are proposed for smoothing the noisy measured temperatures on each analysis sub-time interval before performing the inverse calculation. In addition, $F_1(y,t)$ and $F_2(x,t)$ are also approximated as:

$$F_1(y,t)=\sum_{i=1}^{p}(C_{2(2i-1)-1}+C_{2(2i-1)+1}t)y^{i-1}, \tag{22}$$

$$F_2(x,t)=\sum_{i=1}^{p}(C_{2(2i-1)}+C_{2(2i-1)+2}t)x^{i-1}, \tag{23}$$

where $\{C_1,C_2,\ldots,C_{4p}\}$ are the unknown coefficients and are estimated simultaneously for each analysis interval. The number of thermocouples, J, is equal to $2p$.

The least-squares minimization technique is applied to minimize the sum of the squares of the deviations between the calculated and curve-fitted temperature measurements taken from the ith thermocouple at $t=t_{m-1}$ and $t=t_m$. The error in the estimates $E(C_1,C_2,\ldots,C_{4p})$

$$E(C_1,C_2,\ldots,C_{4p})=\sum_{n=m-1}^{m}\sum_{i=1}^{2p}\left[T_{i,n}^{\mathrm{cal}}-T_{i,n}^{\mathrm{cur}}\right]^2 \quad \text{for } m=1,2,\ldots,M, \tag{24}$$

is to be minimized. $T_{i,n}^{\mathrm{cur}}$, $i=1,2,\ldots,2p$, is obtained from the curve-fitted profile of temperature measurements taken from the ith thermocouple at $t=t_n$. The estimated values of C_j are determined until the value of $E(C_1,C_2,\ldots,C_{4p})$ is minimum. The computational procedures for estimating the unknown coefficients C_j are described as follows.

First, the initial guesses of C_j can be arbitrarily chosen. Accordingly, the calculated temperature taken from the ith thermocouple at the dimensionless time t_n, $T_{i,n}^{\mathrm{cal}}$, can be determined from Eq. (21). Differences between $T_{i,n}^{\mathrm{cur}}$ and $T_{i,n}^{\mathrm{cal}}$ at $t=t_n$ are expressed as

$$e_{i,n}=T_{i,n}^{\mathrm{cal}}-T_{i,n}^{\mathrm{cur}} \quad \text{for } i=1,2,\ldots,2p \text{ and } n=m-1,m. \tag{25}$$

The new calculated temperature $T_{i,n}^{\mathrm{cal},j}$ can be expanded in a first-order Taylor series as

$$T_{i,n}^{\mathrm{cal},j}=T_{i,n}^{\mathrm{cal}}+\sum_{j=1}^{4p}\frac{\partial T_{i,n}}{\partial C_j}\,\mathrm{d}C_j \quad \text{for } i=1,2,\ldots,2p \text{ and } n=m-1,m. \tag{26}$$

To obtain the derivative $\partial T_{i,n}/\partial C_j$, the new estimated coefficient C_j^* is introduced as

$$C_j^*=C_j+d_j\delta_{jk}\quad \text{for } j,k=1,2,\ldots,4p, \tag{27}$$

where $d_j=C_j^*-C_j$ denotes the correction for $j=k$. The symbol δ_{jk} is the Kronecker delta and is defined as

$$\delta_{jk}=\begin{cases}1 & \text{if } j=k,\\ 0 & \text{if } j\neq k.\end{cases}$$

Accordingly, the new calculated temperature $T_{i,n}^{\mathrm{cal},j}$ with respect to C_j^* given by Eq. (27) can be determined from Eq. (21). Differences between $T_{i,n}^{\mathrm{cal},j}$ and $T_{i,n}^{\mathrm{cur}}$ can be written as

$$e_{i,n}^{j}=T_{i,n}^{\mathrm{cal},j}-T_{i,n}^{\mathrm{cur}} \quad \text{for } i=1,2,\ldots,2p \text{ and } n=m-1,m. \tag{28}$$

The finite difference representation of the derivative $\partial T_{i,n}/\partial C_j$ can be expressed as

$$\omega^j_{i,n} = \frac{\partial T_{i,n}}{\partial C_j} = \frac{T^{\mathrm{cal},j}_{i,n} - T^{\mathrm{cal}}_{i,n}}{C^*_j - C_j} \quad \text{for } i = 1,2,\ldots,2p \text{ and } n = m-1, m. \tag{29}$$

The substitution of Eqs. (24), (27) and (28) into Eq. (29) yields

$$\omega^j_{i,n} = \left(e^j_{i,n} - e_{i,n}\right)/d_j \quad \text{for } i = 1,2,\ldots,2p \text{ and } n = m-1, m. \tag{30}$$

Thus Eq. (26) can be rewritten as

$$T^{\mathrm{cal},j}_{i,n} = T^{\mathrm{cal}}_{i,n} + \sum_{j=1}^{4p} \omega^j_{i,n} d^*_j \quad \text{for } i = 1,2,\ldots,2p \text{ and } n = m-1, m, \tag{31}$$

where $d^*_j = \mathrm{d}C_j$ denotes the new correction with respect to the values of C_j.

Substituting Eq. (31) into Eq. (28) in conjunction with Eq. (25) yields

$$e^j_{i,n} = e_{i,n} + \sum_{j=1}^{4p} \omega^j_{i,n} d^*_j \quad \text{for } i = 1,2,\ldots,2p \text{ and } n = m-1, m. \tag{32}$$

As shown in Eq. (24), the error in the estimates $E(C_1 + \Delta C_1,\ C_2 + \Delta C_2, \ldots, C_{4p} + \Delta C_{4p})$ can be expressed as

$$\mathbf{E} = \sum_{n=m-1}^{m} \sum_{i=1}^{2p} (e^j_{i,n})^2. \tag{33}$$

To yield the minimum value of $\mathbf{E}$ with respect to C_j, differentiation of $\mathbf{E}$ with respect to the new correction d^*_j will be performed. Thus the correction equations corresponding to the values of C_j can be expressed as

$$\sum_{j=1}^{4p} \sum_{n=m-1}^{m} \sum_{k=1}^{2p} \omega^i_{k,n} \omega^j_{k,n} d^*_j = -\sum_{n=m-1}^{m} \sum_{j=1}^{2p} \omega^i_{j,n} e_{j,n}, \quad i = 1,2,\ldots,4p. \tag{34}$$

Eq. (34) is a set of $4p$ algebraic equations for the new corrections. The new correction d^*_j can be obtained by solving Eq. (34). Thereafter, the new estimated coefficients can be determined. The above procedures are repeated until the differences between $T^{\mathrm{cur}}_{i,n}$ and $T^{\mathrm{cal}}_{i,n}$ are all less than 10^{-4}.

3. Results and discussion

It can be found from [14] that the present method for estimating the surface temperatures from temperature measurements has very good accuracy. However, to further demonstrate the accuracy and efficiency of this method, the present problem is investigated and a comparison between the present estimates and results given by Yang [10] is also made. All the computations are performed on the PC. The present numerical results are obtained by using $t_0 = 0.1$, $t_f = 0.3$, $M = 10$, $\Delta t_e = 0.02$, $J = 6$, $p = 3$, $n_x = n_y = 11$ and $\ell_x = \ell_y = 0.1$. The initial guess of $\{C_1, C_2, \ldots, C_{12}\}$ is $\{1, 1, \ldots, 1\}$. The unknown boundary conditions shown in [10] are illustrated as follows:

$$T(1, y, t) = F_1(y, t) = 1 + 0.2t + 0.5y + 0.2y^2 + 0.3yt, \tag{35}$$

$$T(x, 0, t) = F_2(x, t) = 1.5 + 0.5t + 0.1x + 0.3x^2 + 0.4xt. \tag{36}$$

Yang [10] applied seven-point measurements to obtain 10 unknown coefficients. In order to validate the present numerical method, the present results obtained by using six-point measurements are compared with those of Yang [10] using seven-point measurements. Yang [10] did not investigate the effect of the measurement locations on the estimates. Thus the present study uses two different sets of the measurement locations to predict the unknown surface temperatures and investigates the effect of the measurement locations on the estimates. Table 1 shows the measurement locations given by the present study and Yang [10]. Six measurement locations of Case A in the present study are chosen from the measurement locations given by Yang [10]. The measurement locations of Case B are farther away from the estimated surface than those listed in the work of Yang [10]. The present problem in [10] can be regarded as an inverse problem of parameter estimation. In other words, the functional forms of the unknown surface temperatures in [10] were given in advance and unknown parameters were estimated by the inverse analysis. But, in the present study, the functional forms of the unknown surface temperatures are unknown a priori. Thus the functional forms, as shown in Eqs. (22) and (23), are applied to estimate the unknown surface temperatures in each analysis sub-time interval.

Figs. 2 and 3 respectively show the comparison of the surface temperature distributions of $T(1, y, 0.15)$ and $T(x, 0, 0.15)$ between the exact results and the present estimated results using the measurement points of Case B shown in Table 1 for $\omega = 0$. Results show that the present numerical scheme has good accuracy even though thermocouples are located far away from the positions of the unknown boundary conditions. It can be found that Yang [10] did not show the inverse solution for larger values of time and only showed the estimates for the small value of time, such as $T(1, y, 0.15)$ and $T(x, 0, 0.15)$. To further evidence the accuracy and efficiency of the present method, a comparison between

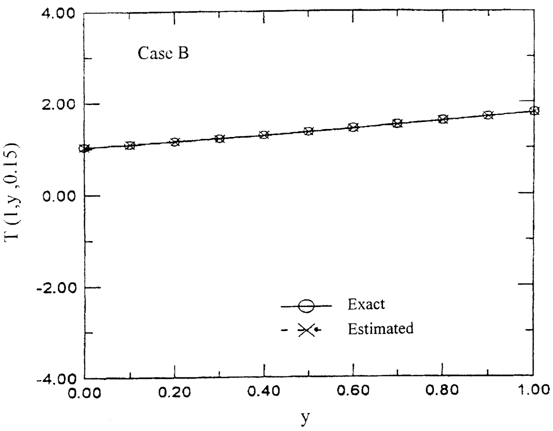

Fig. 2. Comparison of $T(1,y,0.15)$ between the present estimate and exact result for Case B and $\omega = 0$.

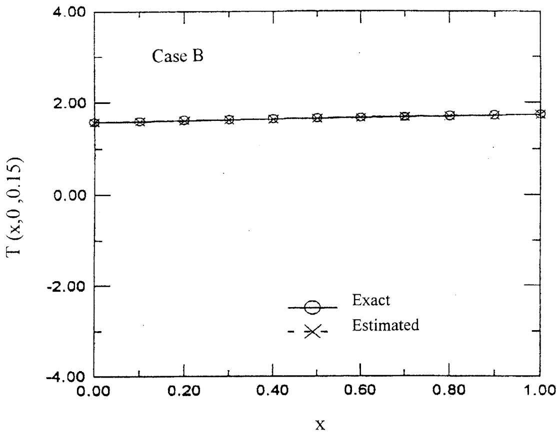

Fig. 3. Comparison of $T(x,0,0.15)$ between the present estimate and exact result for Case B and $\omega = 0$.

the present estimates $T^{est}(x,0,t)$ and $T^{est}(1,y,t)$ using the measurement points of Case B and the exact values for $\omega = 3\%$ and 5% at $t = 0.15$ and 0.3 are shown in Tables 2 and 3. It can be found that the present estimates $T^{est}(x,0,t)$ and $T^{est}(1,y,t)$ are in good agreement with the exact values $T^{exa}(x,0,t)$ and $T^{exa}(1,y,t)$. In addition, the present estimates exhibit stable behavior and do not deviate from the exact results for $\omega = 3\%$ and 5% at $t = 0.15$ and 0.3. This implies that the present estimated values do not change apparently with the measurement locations. The average square error between the estimated values and exact solutions is around 0.1% for $\omega = 0\%$.

The surface temperature distributions of $T(1,y,0.15)$ and $T(x,0,0.15)$ shown in Figs. 4 and 5 are obtained by using the measurement points of Case A shown in Table 1. To investigate the effect of the measurement error on the estimates, a comparison of the surface temperature distributions of $T(1,y,0.15)$ and $T(x,0,0.15)$ between the present estimated results using six thermocouples and the results of Yang [10] using seven thermocouples for various ω values is made, as shown in Figs. 4 and 5. It appears from these figures that the results of Yang [10] exhibit unstable behavior for larger ω values (i.e., $\omega = 3\%$ and 5%) and deviate from the exact results. Conversely, the present estimates perform stable behavior for these ω values at $t = 0.15$. It can be found from Figs. 2, 3, 4(b) and 5(b) that the differences between the exact results and the present estimated results using the measurement locations of

Table 2
Present estimates of $T(x,0,t)$ for various ω and t values with respect to Cases A and B

			x					
			0.0	0.2	0.4	0.6	0.8	1.0
$T^{exa}(x,0,t)$	$t = 0.15$		1.575	1.619	1.687	1.779	1.895	2.035
	$t = 0.3$		1.650	1.706	1.786	1.890	2.018	2.170
$T^{est}(x,0,t)$								
Case A	$t = 0.15$	$\omega = 0\%$	1.574	1.618	1.686	1.779	1.896	2.036
		$\omega = 3\%$	1.586	1.630	1.699	1.791	1.907	2.047
		$\omega = 5\%$	1.581	1.635	1.708	1.798	1.907	2.034
	$t = 0.3$	$\omega = 0\%$	1.640	1.701	1.785	1.890	2.018	2.169
		$\omega = 3\%$	1.650	1.705	1.786	1.892	2.024	2.182
		$\omega = 5\%$	1.644	1.682	1.756	1.866	2.012	2.194
Case B	$t = 0.15$	$\omega = 0\%$	1.560	1.621	1.694	1.780	1.879	1.990
		$\omega = 3\%$	1.556	1.622	1.693	1.767	1.846	1.928
		$\omega = 5\%$	1.547	1.624	1.699	1.773	1.846	1.918
	$t = 0.3$	$\omega = 0\%$	1.645	1.707	1.788	1.887	2.006	2.144
		$\omega = 3\%$	1.645	1.706	1.786	1.886	2.004	2.142
		$\omega = 5\%$	1.643	1.705	1.785	1.886	2.005	2.144

Table 3
Present estimates of $T(1,y,t)$ for various ω and t values with respect to Cases A and B

			y					
			0.0	0.2	0.4	0.6	0.8	1.0
$T^{exa}(1,y,t)$	$t=0.15$		1.030	1.147	1.280	1.429	1.594	1.775
	$t=0.3$		1.060	1.186	1.328	1.486	1.660	1.850
$T^{est}(1,y,t)$								
Case A	$t=0.15$	$\omega=0\%$	1.024	1.146	1.280	1.428	1.589	1.764
		$\omega=3\%$	1.032	1.148	1.280	1.430	1.597	1.781
		$\omega=5\%$	1.027	1.156	1.296	1.448	1.612	1.787
	$t=0.3$	$\omega=0\%$	1.057	1.185	1.328	1.485	1.657	1.843
		$\omega=3\%$	1.070	1.190	1.327	1.483	1.658	1.851
		$\omega=5\%$	1.072	1.178	1.306	1.457	1.629	1.824
Case B	$t=0.15$	$\omega=0\%$	1.049	1.159	1.287	1.431	1.593	1.773
		$\omega=3\%$	0.992	1.156	1.311	1.458	1.595	1.724
		$\omega=5\%$	1.141	1.195	1.288	1.419	1.590	1.799
	$t=0.3$	$\omega=0\%$	1.053	1.190	1.338	1.494	1.661	1.836
		$\omega=3\%$	1.046	1.186	1.335	1.493	1.660	1.835
		$\omega=5\%$	1.047	1.185	1.333	1.490	1.659	1.837

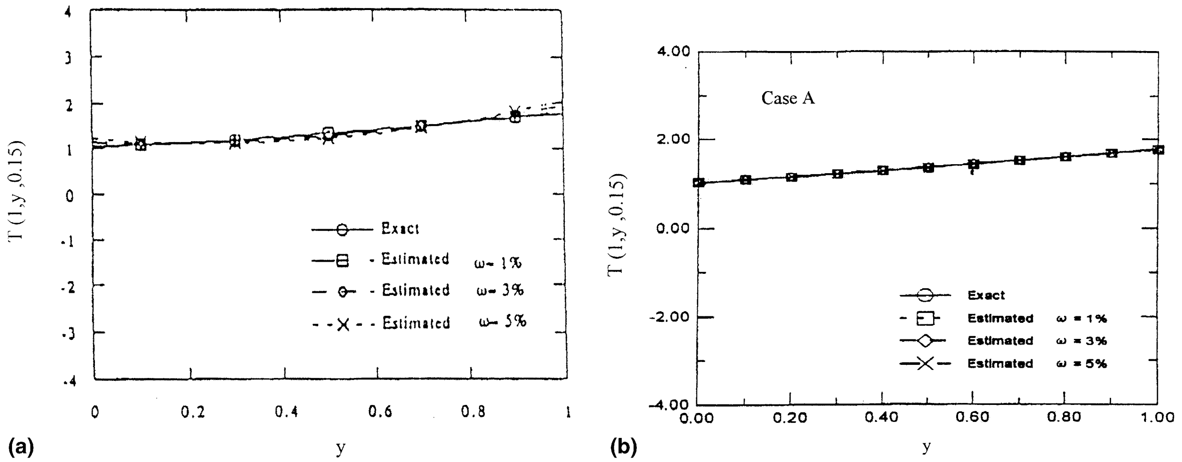

Fig. 4. (a) Comparison of $T(1,y,0.15)$ between exact results and estimates of Yang [10] for Case A and various ω values. (b) Comparison of $T(1,y,0.15)$ between present estimates and exact results for Case A and various ω values.

Case A and Case B are small. The foregoing comparison further shows that the effect of the measurement locations on the estimates is small for the present method.

We also apply other three different sets of the initial guesses, such as $\{C_1, C_2, \ldots, C_{12}\} = \{0.5, 0.5, \ldots, 0.5\}$, $\{0.8, 0.8, \ldots, 0.8\}$ and $\{2, 2, \ldots, 2\}$, to predict the unknown surface temperatures $T(1,y,t)$ and $T(x,0,t)$. Their results are not shown in this manuscript because they agree well with those using the initial guess of $\{1, 1, \ldots, 1\}$. The above statements imply that the effect of the initial guesses on the accuracy of the estimates is not significant for the present method.

4. Conclusions

The hybrid application of the Laplace transform and the FDM in conjunction with the least-squares scheme and a sequential-in-time concept is successfully applied to estimate the unknown surface temperatures from temperature data measured at any location in a plate. The functional form of the unknown surface temperatures is unknown a priori. Owing to the application of the Laplace transform, the present method is not a time-stepping procedure. Thus the unknown surface temperature distributions at any specific analysis subtime interval can be predicted from the temperature

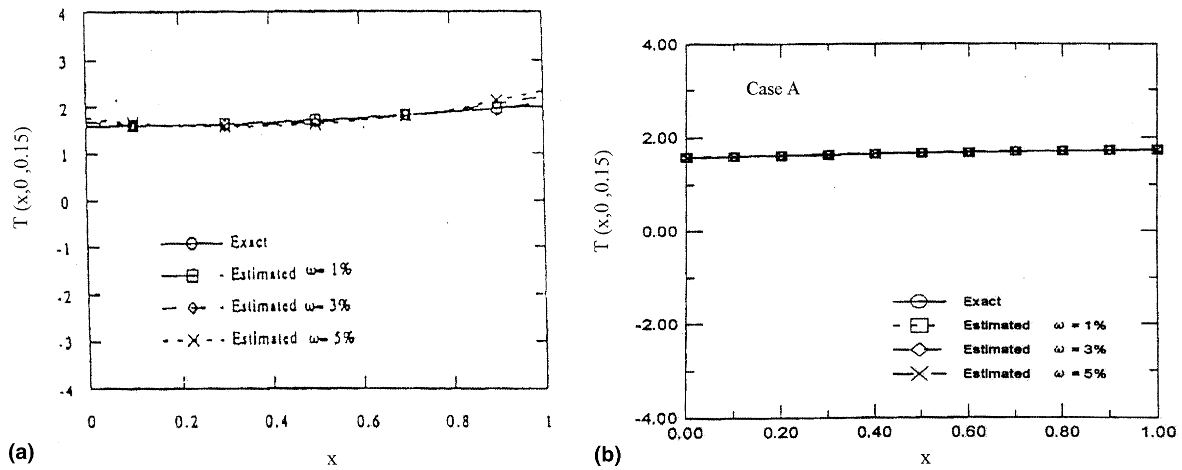

Fig. 5. (a) Comparison of $T(x, 0, 0.15)$ between exact results and estimates of Yang [10] for Case A and various ω values. (b) Comparison of $T(x, 0, 0.15)$ between present estimates and exact results for Case A and various ω values.

measurements inside the plate without any step-by-step computations from $t = t_0$. The present estimates exhibit stable behavior for various ω values and agree with the exact results even though measuring points are located far from the positions of the estimates. Results also show that the effect of the initial guesses on the accuracy of the estimates is not significant for the present method. A small effect of the measurement locations on the estimates can be observed from the present study. This implies that the present hybrid method offers a great deal of flexibility for the inverse heat conduction problems.

References

[1] M.N. Özisik, Heat Conduction, second ed., Wiley, New York, 1993 (Chapter 14).

[2] E.M. Sparrow, A. Haji-Sheikh, T.S. Lundgern, The inverse problem in transient heat conduction, J. Appl. Mech. 86 (1964) 369–375.

[3] K.W. Woo, L.C. Chow, Inverse heat conduction by direct inverse Laplace transform, Numer. Heat Transfer 4 (1981) 499–504.

[4] M. Monde, Analytical method in inverse heat transfer problem using Laplace transform technique, Int. J. Heat Mass Transfer 43 (2000) 3965–3975.

[5] M. Imber, Two-dimensional inverse conduction problem – further observation, AIAA J. 13 (1975) 114–115.

[6] H.R. Busby, D.M. Trujillo, Numerical solution to a two-dimensional inverse heat conduction problem, Int. J. Numer. Methods Eng. 21 (1985) 349–359.

[7] G.W. Krutz, R.J. Schoenhals, P.S. Hore, Application of the finite element method to the inverse heat conduction problem, Numer. Heat Transfer 1 (1978) 489–498.

[8] N. Zabaras, J.C. Liu, An analysis of two-dimensional linear heat transfer problems using an integral method, Numer. Heat Transfer 13 (1988) 527–533.

[9] C.Y. Yang, C.K. Chen, The boundary estimation in two-dimensional inverse heat conduction problems, J. Phys. D 29 (1996) 333–339.

[10] C.Y. Yang, Symbolic computation to estimate two-sided boundary conditions in two-dimensional conduction problems, J. Thermophys. Heat Transfer 10 (1996) 1–5.

[11] C.Y. Yang, Inverse estimation of mixed-typed boundary conditions in heat conduction problems, J. Thermophys. Heat Transfer 12 (1998) 552–561.

[12] P.T. Hsu, Y.T. Yang, C.K. Chen, Simultaneously estimating the initial and boundary conditions in a two-dimensional hollow cylinder, Int. J. Heat Mass Transfer 41 (1998) 218–227.

[13] H.T. Chen, S.M. Chang, Application of the hybrid method to inverse heat conduction problems, Int. J. Heat Mass Transfer 33 (1990) 621–628.

[14] H.T. Chen, S.Y. Lin, L.C. Fang, Estimation of surface temperature in two-dimensional inverse heat conduction problems, Int. J. Heat Mass Transfer 44 (2001) 1455–1463.

[15] H.T. Chen, J.Y. Lin, C.H. Wu, C.H. Huang, Numerical algorithm in estimating the temperature-dependent thermal conductivity, Numer. Heat Transfer 29 (B) (1996) 509–522.

[16] H.T. Chen, J.Y. Lin, Simultaneous estimations of temperature-dependent thermal conductivity and heat capacity, Int. J. Heat Mass Transfer 41 (1998) 1144–2273.

[17] J.P. Holman, W.J. Gajda Jr., in: Experimental Methods for Engineers, McGraw-Hill, New York, 1989, pp. 37–83.

[18] H.T. Chen, J.Y. Lin, Hybrid Laplace transform technique for non-linear transient thermal problems, Int. J. Heat Mass Transfer 34 (1991) 1301–1308.

[19] H.T. Chen, J.Y. Lin, Numerical analysis for hyperbolic heat conduction, Int. J. Heat Mass Transfer 36 (1993) 2891–2898.

[20] G. Honig, U. Hirdes, A method for the numerical inversion of Laplace transforms, J. Comput. Appl. Math. 10 (1984) 113–132.